

Lecture 19: Longitudinal Dynamics

The small perturbation equations describing the stick-fixed longitudinal motion of an airplane are

$$\dot{\bar{\mathbf{x}}}_L = \bar{\mathbf{A}}_L \bar{\mathbf{x}}_L + \bar{\mathbf{B}}_L \bar{\mathbf{u}}_L$$

where the reduced longitudinal state vector and input vector are

$$\bar{\mathbf{x}}_L = \begin{pmatrix} \Delta u \\ \Delta w \\ \Delta q \\ \Delta \theta \end{pmatrix}, \quad \text{and} \quad \bar{\mathbf{u}}_L = \begin{pmatrix} \Delta \delta e \\ \Delta \delta T \end{pmatrix},$$

the reduced longitudinal state matrix is

$$\bar{\mathbf{A}}_L = \begin{pmatrix} \frac{1}{m} X_u & \frac{1}{m} X_w & 0 & -g \\ \frac{Z_u}{m-Z_{\dot{w}}} & \frac{Z_w}{m-Z_{\dot{w}}} & \frac{(Z_q+mu_0)}{m-Z_{\dot{w}}} & 0 \\ \frac{1}{I_y} \left(M_u + \frac{M_{\dot{w}} Z_u}{m-Z_{\dot{w}}} \right) & \frac{1}{I_y} \left(M_w + \frac{M_{\dot{w}} Z_w}{m-Z_{\dot{w}}} \right) & \frac{1}{I_y} \left(M_q + \frac{M_{\dot{w}} (Z_q+mu_0)}{m-Z_{\dot{w}}} \right) & 0 \\ 0 & 0 & 1 & 0 \end{pmatrix}, \quad (1)$$

and the reduced longitudinal input matrix is

$$\bar{\mathbf{B}}_L = \begin{pmatrix} \frac{1}{m} X_{\delta e} & \frac{1}{m} X_{\delta T} \\ \frac{Z_{\delta e}}{m-Z_{\dot{w}}} & \frac{Z_{\delta T}}{m-Z_{\dot{w}}} \\ \frac{1}{I_y} \left(M_{\delta e} + \frac{M_{\dot{w}} Z_{\delta e}}{m-Z_{\dot{w}}} \right) & \frac{1}{I_y} \left(M_{\delta T} + \frac{M_{\dot{w}} Z_{\delta T}}{m-Z_{\dot{w}}} \right) \\ 0 & 0 \end{pmatrix}. \quad (2)$$

To begin, we consider only the *stick-fixed* motion, i.e., the initial condition response to small perturbations in which the controls are held constant at their nominal, equilibrium values: $\bar{\mathbf{u}}_L = \mathbf{0}$.

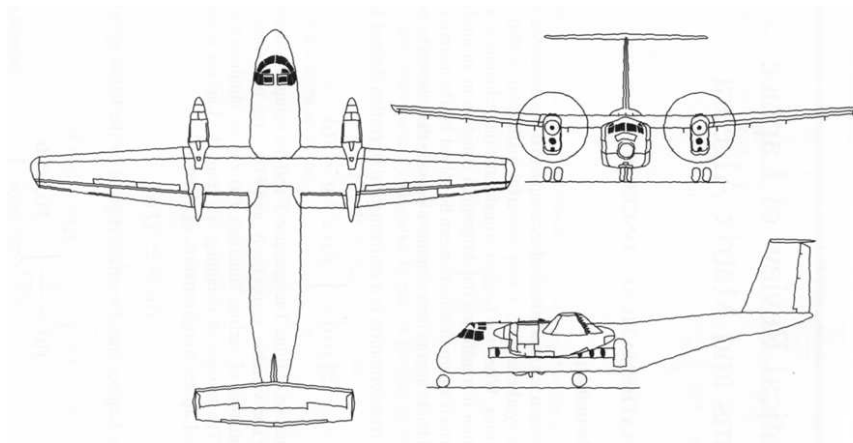


Figure 1: A short takeoff and landing airplane [1].

Stick-Fixed, Longitudinal Response of a STOL Airplane. Consider the STOL aircraft shown in Figure 1.

$$W = 40,000 \text{ lb} \quad (m = 1242.2 \text{ slug}), \quad I_y = 215,000 \text{ slug ft}^2, \quad S = 945 \text{ ft}^2, \quad \bar{c} = 10.1 \text{ ft}.$$

For constant altitude, wings level flight at speed 400 ft/s and altitude 10,000 ft, the relevant stability derivatives are

	$X_{(\cdot)}$	$Z_{(\cdot)}$	$M_{(\cdot)}$
u	$-35.7 \text{ lb}/(\text{ft}/\text{s})$	$-200.7 \text{ lb}/(\text{ft}/\text{s})$	$0 \text{ (ft lb)}/(\text{ft}/\text{s})$
w	$-121.2 \text{ lb}/(\text{ft}/\text{s})$	$-1744.7 \text{ lb}/(\text{ft}/\text{s})$	$-2.6 \cdot 10^3 \text{ (ft lb)}/(\text{ft}/\text{s})$
q	$0 \text{ lb}/(\text{rad}/\text{s})$	$-13.1 \cdot 10^3 \text{ lb}/(\text{rad}/\text{s})$	$-600.4 \text{ (ft lb)}/(\text{rad}/\text{s})$
\dot{w}	$0 \text{ lb}/(\text{ft}/\text{s}^2)$	$-5.6 \text{ lb}/(\text{ft}/\text{s}^2)$	$-256.0 \text{ (ft lb)}/(\text{ft}/\text{s}^2)$

We find that the eigenvalues and corresponding eigenvectors for $\bar{\mathbf{A}}_L$ are

$$\lambda_{1,2} = -2.3297 \pm 1.7818j \quad \text{with} \quad \mathbf{v}_{1,2} = \begin{pmatrix} -0.0456 \\ -0.9986 \\ 0.0024 \\ -0.0016 \end{pmatrix} \pm j \begin{pmatrix} -0.0248 \\ 0 \\ -0.0046 \\ 0.0008 \end{pmatrix}$$

and

$$\lambda_{3,4} = -0.0102 \pm 0.0848j \quad \text{with} \quad \mathbf{v}_{3,4} = \begin{pmatrix} 0.9986 \\ -0.0523 \\ 0.0002 \\ -0.0004 \end{pmatrix} \pm j \begin{pmatrix} 0 \\ 0.0008 \\ -0.0000 \\ -0.0026 \end{pmatrix}.$$

The real part of the eigenvalues λ_1 and λ_2 (the $-\zeta\omega_n$ component) is comparatively large, meaning that the contribution of these terms to the initial condition response varies rapidly. Also, the ratio of the imaginary part to the real part is smaller meaning that these terms contribute fairly well-damped oscillations. The eigenvalues λ_1 and λ_2 correspond to the “short-period” mode. This mode is governed largely by the size and location of the horizontal tail. It is the more critical mode in terms of longitudinal stability. The short period natural frequency and damping ratio are

$$\omega_{n_{\text{sp}}} = 2.93 \text{ rad/s} \quad \text{and} \quad \zeta_{\text{sp}} = 0.79.$$

The time and number of cycles to half amplitude for this well-damped, stable mode are

$$t_{\text{half}_{\text{sp}}} = 0.30 \text{ s} \quad \text{and} \quad N_{\text{half}_{\text{sp}}} = 0.08.$$

The real part of the eigenvalues λ_3 and λ_4 (the “ $-\zeta\omega_n$ ” component) is relatively small in magnitude, meaning that the contribution of these terms to the initial condition response varies slowly. Also, the ratio of the imaginary part to the real part is fairly large meaning that these terms contribute underdamped oscillations. The eigenvalues λ_3 and λ_4 correspond to the “long-period” or “phugoid” mode. This mode is characterized by a relatively slow trade-off between kinetic energy (speed) and potential energy (altitude). The phugoid natural frequency and damping ratio are

$$\omega_{n_{\text{p}}} = 0.085 \text{ rad/s} \quad \text{and} \quad \zeta_{\text{p}} = 0.12.$$

The time and number of cycles to half amplitude for this lightly damped, stable mode are

$$t_{\text{half}_{\text{p}}} = 68 \text{ s} \quad \text{and} \quad N_{\text{half}_{\text{p}}} = 0.91.$$

Phugoid Mode Approximation. While it is possible to formally compute eigenvalues and eigenvectors analytically, without substituting values for parameters, it is much more convenient and insightful to obtain simple approximations which capture the essential physics. Suppose, then, that we wish to approximate the phugoid mode. To do so, we must isolate this lightly damped, long period mode from the general transient response. Note that one characteristic of the short period response is that $\Delta\alpha$ converges quickly to zero, or very nearly so. Using this observation, in a previous lecture, we approximated the phugoid mode by assuming that $\Delta w \equiv 0$. We also neglected Z_q and $Z_{\dot{w}}$. For the STOL aircraft in Figure 1, the

magnitude of Z_q is only 3% of mu_0 while the magnitude of $Z_{\dot{w}}$ is 0.5% of m . Referring to $\bar{\mathbf{A}}_L$ in (1), it is clear that we can neglect these terms.

The resulting approximation was

$$\omega_{n_p} \approx \sqrt{-\frac{Z_u g}{m u_0}} \quad \text{and} \quad \zeta_p \approx -\frac{X_u}{2m\omega_{n_p}}.$$

For the STOL example above, this approximation gives

$$\omega_{n_p} \approx 0.11 \text{ rad/s} \quad \text{and} \quad \zeta_p \approx 0.12.$$

Comparing this approximation with the actual values computed earlier, we see that the damping ratio approximation is quite accurate, although the natural frequency is slightly over-estimated.

Short Period Mode Approximation. As we have seen, a good approximation of the Phugoid mode may be obtained by assuming that $\Delta\alpha \equiv 0$. This assumption allows us to express the mode in terms of the variables Δu and $\Delta\theta$. It stands to reason, then, that the short period mode should involve the remaining two variables Δw and Δq . Specifically, if we assume that $\Delta u = 0$ and ignore the pitch angle $\Delta\theta$, we obtain the equations

$$\begin{pmatrix} \Delta\dot{w} \\ \Delta\dot{q} \end{pmatrix} = \begin{pmatrix} \frac{1}{I_y} (M_w + \frac{1}{m} M_{\dot{w}} Z_w) & u_0 \\ \frac{1}{I_y} (M_q + M_{\dot{w}} u_0) & \end{pmatrix} \begin{pmatrix} \Delta w \\ \Delta q \end{pmatrix}.$$

The characteristic polynomial for the system above is

$$\lambda^2 - \left[\frac{1}{m} Z_w + \frac{1}{I_y} (M_q + u_0 M_{\dot{w}}) \right] \lambda + \left[\frac{1}{m I_y} Z_w M_q - \frac{u_0}{I_y} M_w \right].$$

The coefficient of λ^1 is positive because Z_w , M_q and $M_{\dot{w}}$ are all negative. Because M_w is negative, as well, the coefficient of λ^0 is also positive. Thus, we may write

$$2\zeta_{sp}\omega_{n_{sp}} \approx - \left[\frac{1}{m} Z_w + \frac{1}{I_y} (M_q + u_0 M_{\dot{w}}) \right]$$

and

$$\omega_{n_{sp}}^2 \approx \frac{1}{m I_y} Z_w M_q - \frac{u_0}{I_y} M_w.$$

The approximate short period natural frequency and damping ratio are

$$\omega_{n_{sp}} \approx \sqrt{\frac{1}{m I_y} Z_w M_q - \frac{u_0}{I_y} M_w} \quad \text{and} \quad \zeta_{sp} \approx -\frac{1}{2\omega_{n_{sp}}} \left[\frac{1}{m} Z_w + \frac{1}{I_y} (M_q + u_0 M_{\dot{w}}) \right].$$

For the STOL example given previously, the approximation above gives

$$\omega_{n_{sp}} \approx 2.96 \text{ rad/s} \quad \text{and} \quad \zeta_{sp} \approx 0.79.$$

These values agree quite well with the true values computed from the complete state matrix.

Figure 2 illustrates the effect of various longitudinal parameters on modal frequencies and damping ratios. The key parameters affecting the short period mode are the pitch stiffness and the pitch damping. Both of these values are determined, in large part, by the horizontal tail volume ratio. Key parameters affecting the phugoid mode include speed and lift-to-drag ratio. Note that, while the tail volume may be considered

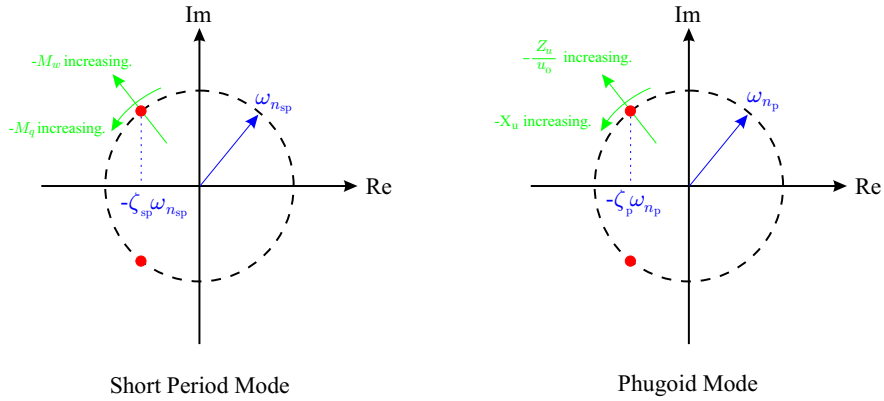


Figure 2: Effect of key parameters on longitudinal modes.

a free design parameter, the cruise speed and lift-to-drag ratio are typically dictated by basic customer requirements.

Performance Specifications: Flying Qualities. The term “flying qualities” is a seemingly vague reference to the overall “feel” of an airplane. In fact, a considerable amount of effort has gone into developing a firm and quantifiable definition of this term. The Cooper-Harper Pilot Opinion Rating Scale is a questionnaire developed for test pilots in order to quantify their opinions about the aircraft that they fly. Essentially, a pilot rates an airplane’s performance on a scale of one to ten, with one representing “excellent, highly desirable” performance characteristics and with ten representing “major deficiencies” in performance. This rating can be related to the following three levels of flying qualities:

- Level 1: Flying qualities clearly adequate for the mission flight phase.
- Level 2: Flying qualities adequate to accomplish the mission flight phase but some increase in pilot workload or degradation in mission effectiveness exists.
- Level 3: Flying qualities such that the airplane can be controlled safely, but pilot workload is excessive or mission effectiveness is inadequate or both.

Using the Cooper-Harper scale, these three levels of flying qualities have in turn been related to formal numerical bounds on the parameters that characterize an airplane’s dynamics, such as short period and phugoid natural frequency and damping ratio. As a basic requirement, the short period mode must be dynamically stable. Table 1, adapted from [1], shows bounds on the short period damping ratio for two representative flight phases and the three flying quality levels.

Table 1: Bounds on ζ_{sp} .

	Take-off & Landing		Cruising Flight	
Level	min	max	min	max
1	0.35	1.30	0.30	2.00
2	0.25	2.00	0.20	2.00
3	0.15	-	0.15	-

Better still, Figure 3 shows a “thumbprint plot” of short period natural frequencies and damping ratios. The center of the contour marked “Good” corresponds roughly to a natural frequency of π radians per second and a damping ratio of $\frac{\sqrt{2}}{2}$.

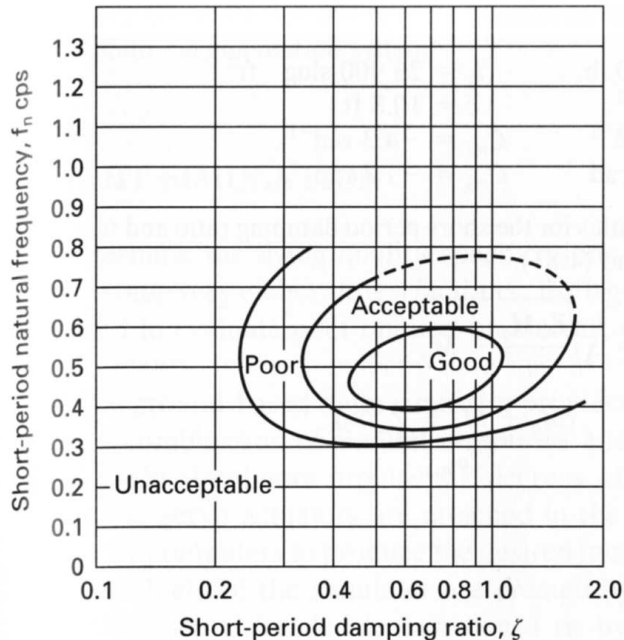


Figure 3: Short period natural frequency versus damping ratio [1].

The phugoid mode plays a much less important role in an airplane’s dynamics. Table 2, also adapted from [1], shows bounds on the phugoid damping ratio for the three flying quality levels. Notice that, at least for Level 3 flying qualities, an unstable phugoid mode is acceptable.

Table 2: Bounds on ζ_p .

Level	Condition
1	$\zeta_p > 0.04$
2	$\zeta_p > 0$
3	$t_{\text{double}_p} > 55 \text{ s}$

Longitudinal Step Response of a STOL Airplane. Next, we consider what happens when $\Delta\delta e$ or $\Delta\delta T$ is varied. As a representative case, we will consider step inputs in elevator angle and thrust. The δe derivatives appearing in the matrix $\bar{\mathbf{B}}_L$ given in (2) depend on the elevator effectiveness and the elevator power expressions ($C_{L_{\delta e}}$ and $C_{m_{\delta e}}$) that we developed early in the course. The δT derivatives are really functions of the propulsion system and must be determined case by case. For simplicity, we will typically assume that $Z_{\delta T}$ and $M_{\delta T}$ are zero. (In fact, engines are often installed at a slight incidence to provide additional propulsive lift, which would contribute to both $Z_{\delta T}$ and $M_{\delta T}$, but we will ignore this effect here.) The term $X_{\delta T}$ is somewhat ambiguous. For starters, it is not entirely clear what a “unit” step input in throttle corresponds to. If the unit of throttle displacement is small, one would expect a correspondingly small change in thrust, relative to the aircraft’s weight. In examples, we will *arbitrarily* assume that $X_{\delta T} = 0.1W$; please note, however, that this assumption is completely without physical motivation.

Matlab contains a number of tools for dealing with LTI systems and for transferring between various representations. For example, the Matlab command `ss` takes the matrices \mathbf{A} , \mathbf{B} , \mathbf{C} , and \mathbf{D} as arguments and generates an object called a “system” which is simply the state-space representation. This object can be operated on using commands such as `step` (to obtain the system’s step response) or `initial` (to obtain

the initial condition response). The command `lsim` provides the system response to initial conditions and a user-defined input signal. Having defined a system in state-space form using `ss`, one may determine the system's transfer function matrix using the command `ss2tf`.

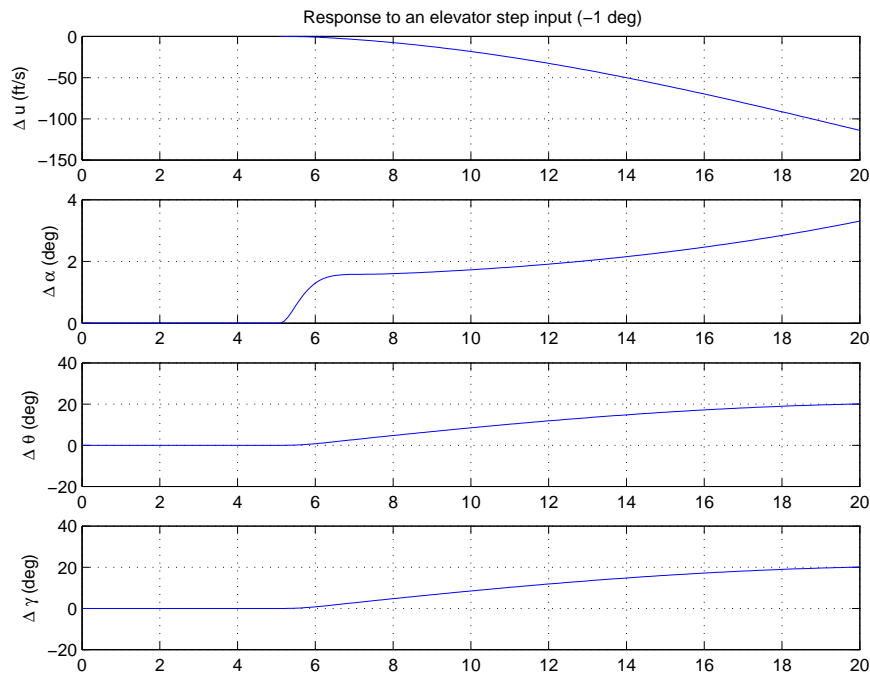


Figure 4: Elevator step response for a STOL airplane [1].

Figure 4 shows the short-term elevator step response for the short takeoff and landing aircraft we have considered in previous lectures. The figure shows four plots representing change in speed Δu , change in angle of attack $\Delta\alpha$, change in pitch angle $\Delta\theta$, and change in flight path angle $\Delta\gamma = \Delta\theta - \Delta\alpha$. The system begins at equilibrium but experiences a -1° elevator deflection at $t = 5$ seconds. Recall that, by convention, a negative elevator deflection gives a nose-up moment. Shortly after the command is executed, the angle of attack “converges” to a small positive value. The time required for this convergence is related to the time constant for the short period mode. Thus, we see that the stick-fixed dynamics impact control characteristics. Also notice that the airplane’s speed begins to drop, and the pitch (and flight path) angle begins to rise.

Over a longer period, as shown in Figure 5, the system undergoes a phugoid-like convergence to a new *horizontal* equilibrium flight condition in which the airplane travels slower and at a correspondingly higher angle of attack.

Next, consider the effect of a unit increase in thrust. As shown in Figure 6, the long-term effect is not an increase in speed u or the angle of attack α , but rather an increase in pitch angle (and thus in flight path angle). That is, the long-term effect of an increase in throttle is for the aircraft to climb at its trim speed and lift coefficient.

References

- [1] R. C. Nelson. *Flight Stability and Automatic Control*. WCB McGraw-Hill, New York, NY, second edition, 1998.

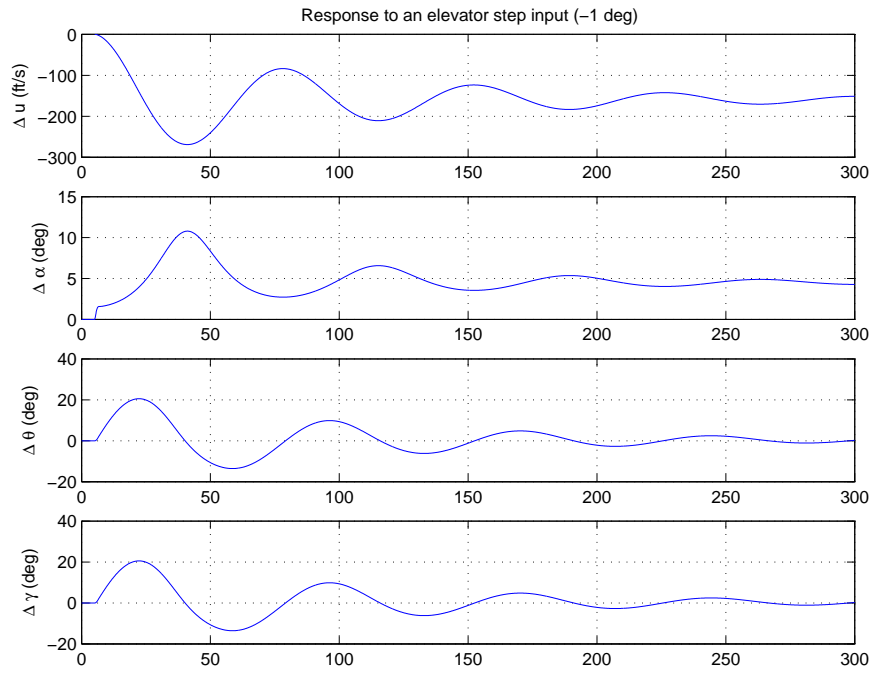


Figure 5: Long-term elevator step response.

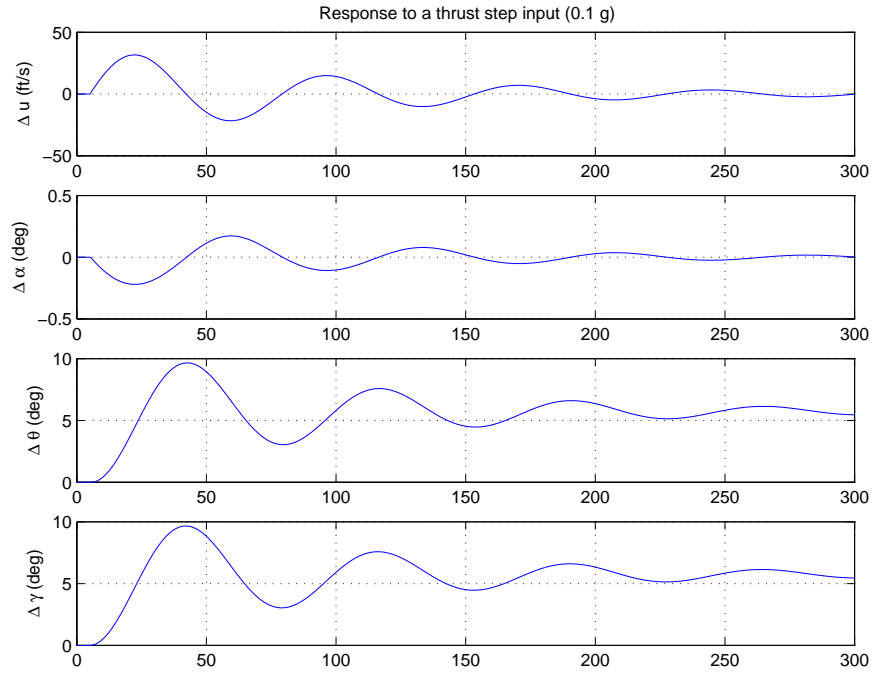


Figure 6: Thrust step response.